Proceedings of the 3rd IASME/WSEAS Int. Conf. on FLUID DYNAMICS & AERODYNAMICS, Corfu, Greece, August 20-22, 2005 (pp59-67)

Modified Theories of Axi-Symmetric Stagnation-Point Laminar Boundary Layer Flow and Counterflow Finite Jets

SIAVASH H. SOHRAB
Robert McCormick School of Engineering and Applied Science
Department of Mechanical Engineering
Northwestern University, Evanston, Illinois 60208
UNITED STATES OF AMERICA
s-sohrab@northwestern.edu
http://www.mech.northwestern.edu/dept/people/faculty/sohrab.html

Abstract: - Scale-invariant forms of mass, energy, and linear momentum conservation equations in chemically reactive fields are described. The modified equation of motion is then solved for the classical problems of axi-symmetric stagnation-point laminar boundary layer flow as well as laminar counterflow finite jets. The results are shown to be in agreement with the classical solutions of *Homann* and *Frössling* as well as the observations.

Key-Words: - Theory of laminar axi-symmetric stagnation-point flow. Theory of counterflow finite jets.

1 Introduction

The universality of turbulent phenomena from stochastic quantum fields to classical hydrodynamic fields resulted in recent introduction of a scale-invariant model of statistical mechanics and its application to the field of thermodynamics [4]. The implications of the model to the study of transport phenomena and invariant forms of conservation equations have also been addressed [5, 6]. In the present study, the modified equation of motion is solved for the classical problems of laminar flow within boundary layer of axi-symmetric stagnation-point and outside of the free-viscous-layer at the stagnation plane of an axi-symmetric finite-jet counterflow. The resulting analytical solutions are found to be in excellent qualitative agreement with the exact numerical calculations based on the classical equation of motion as well as observations.

2 Scale-Invariant Form of the Conservation Equations for Reactive Fields

Following the classical methods [1-3], the invariant definitions of the density ρ_β, and the velocity of *atom* $\mathbf{u}_\beta$, *element* $\mathbf{v}_\beta$, and *system* $\mathbf{w}_\beta$ at the scale β are given as [4]

$$\rho_\beta = n_\beta m_\beta = m_\beta \int f_\beta du_\beta \quad , \quad \mathbf{u}_\beta = \mathbf{v}_{\beta-1} \qquad (1)$$

$$\mathbf{v}_\beta = \rho_\beta^{-1} m_\beta \int \mathbf{u}_\beta f_\beta d\mathbf{u}_\beta \quad , \quad \mathbf{w}_\beta = \mathbf{v}_{\beta+1} \qquad (2)$$

Also, the invariant definitions of the peculiar and the diffusion velocities are given as [4]

$$\mathbf{V}'_\beta = \mathbf{u}_\beta - \mathbf{v}_\beta \quad , \quad \mathbf{V}_\beta = \mathbf{v}_\beta - \mathbf{w}_\beta = \mathbf{V}'_{\beta+1} \qquad (3)$$

Next, following the classical methods [1-3], the scale-invariant forms of mass, thermal energy, and linear momentum conservation equations at scale β are given as [5, 6]

$$\frac{\partial \rho_\beta}{\partial t} + \nabla.\left(\rho_\beta \mathbf{v}_\beta\right) = \Omega_\beta \qquad (4)$$

$$\frac{\partial \varepsilon_\beta}{\partial t} + \nabla.\left(\varepsilon_\beta \mathbf{v}_\beta\right) = 0 \qquad (5)$$

$$\frac{\partial \mathbf{p}_\beta}{\partial t} + \nabla.\left(\mathbf{p}_\beta \mathbf{v}_\beta\right) = 0 \qquad (6)$$

involving the *volumetric density* of thermal energy $\varepsilon_\beta = \rho_\beta h_\beta$ and linear momentum $\mathbf{p}_\beta = \rho_\beta \mathbf{v}_\beta$. Also, Ω_β is the chemical reaction rate and h_β is the absolute enthalpy.

The local velocity $\mathbf{v}_\beta$ in (4)-(6) is expressed in terms of the convective $\mathbf{w}_\beta = \langle \mathbf{v}_\beta \rangle$ and diffusive the $\mathbf{V}_\beta$ velocities [5]

$$\mathbf{v}_\beta = \mathbf{w}_\beta + \mathbf{V}_{\beta g} \quad , \quad \mathbf{V}_{\beta g} = -D_\beta \nabla \ln(\rho_\beta) \qquad (7a)$$

$$\mathbf{v}_\beta = \mathbf{w}_\beta + \mathbf{V}_{\beta tg} \quad , \quad \mathbf{V}_{\beta tg} = -\alpha_\beta \nabla \ln(\varepsilon_\beta) \qquad (7b)$$

$$\mathbf{v}_\beta = \mathbf{w}_\beta + \mathbf{V}_{\beta hg} \quad , \quad \mathbf{V}_{\beta hg} = -\nu_\beta \nabla \ln(\mathbf{p}_\beta) \qquad (7c)$$

where ($\mathbf{V}_{\beta g}$, $\mathbf{V}_{\beta tg}$, $\mathbf{V}_{\beta hg}$) are respectively the diffusive, the thermo-diffusive, the linear hydro-diffusive velocities. The hierarchy of statistical fields from molecular-dynamics to eddy-dynamics is schematically shown in Fig.1.

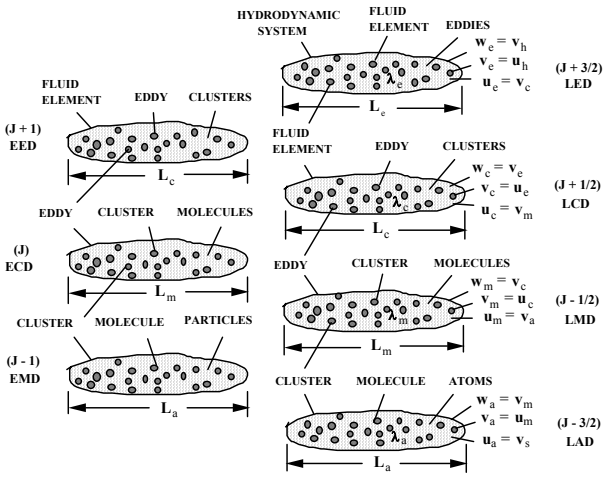

Fig.1 Hierarchy of statistical fields for equilibrium eddy-, cluster-, and molecular-dynamic scales and the associated laminar flow fields.

For unity *Schmidt* and *Prandtl* numbers, one may express

$$\mathbf{V}_{\beta tg} = \mathbf{V}_{\beta g} + \mathbf{V}_{\beta t} \quad , \quad \mathbf{V}_{\beta t} = -\alpha_\beta \nabla \ln(h_\beta) \tag{8a}$$

$$\mathbf{V}_{\beta hg} = \mathbf{V}_{\beta g} + \mathbf{V}_{\beta h} \quad , \quad \mathbf{V}_{\beta h} = -\nu_\beta \nabla \ln(\mathbf{v}_\beta) \tag{8b}$$

that involve the thermal $\mathbf{V}_{\beta t}$, and linear hydrodynamic $\mathbf{V}_{\beta h}$ diffusion velocities [5]. Since for an ideal gas $h_\beta = c_{p\beta} T_\beta$, when $c_{p\beta}$ is constant and $T = T_\beta$, Eq.(8a) reduces to the *Fourier* law of heat conduction

$$\mathbf{q}_\beta = \rho_\beta h_\beta \mathbf{V}_{\beta t} = -\kappa_\beta \nabla T \tag{9}$$

where κ_β and $\alpha_\beta = \kappa_\beta / (\rho_\beta c_{p\beta})$ are the thermal conductivity and diffusivity. Similarly, (8b) may be identified as the shear stress associated with diffusional flux of linear momentum and expressed by the generalized *Newton* law of viscosity [5]

$$\boldsymbol{\tau}_{ij\beta} = \rho_\beta \mathbf{v}_{j\beta} \mathbf{V}_{ij\beta h} = -\mu_\beta \partial \mathbf{v}_{j\beta} / \partial \mathbf{x}_i \tag{10}$$

Substitutions from (7a)-(7c) into (4)-(6), neglecting cross-diffusion terms and assuming constant transport coefficients with $Sc_\beta = Pr_\beta = 1$, result in [5, 6]

$$\frac{\partial \rho_\beta}{\partial t} + \mathbf{w}_\beta . \nabla \rho_\beta - D_\beta \nabla^2 \rho_\beta = \Omega_\beta \tag{11}$$

$$h_\beta \left[\frac{\partial \rho_\beta}{\partial t} + \mathbf{w}_\beta . \nabla \rho_\beta - D_\beta \nabla^2 \rho_\beta \right] + \rho_\beta \left[\frac{\partial h_\beta}{\partial t} + \mathbf{w}_\beta . \nabla h_\beta - \alpha_\beta \nabla^2 h_\beta \right] = 0 \tag{12}$$

$$\mathbf{v}_\beta \left[\frac{\partial \rho_\beta}{\partial t} + \mathbf{w}_\beta . \nabla \rho_\beta - D_\beta \nabla^2 \rho_\beta \right] + \rho_\beta \left[\frac{\partial \mathbf{v}_\beta}{\partial t} + \mathbf{w}_\beta . \nabla \mathbf{v}_\beta - \nu_\beta \nabla^2 \mathbf{v}_\beta \right] = 0 \tag{13}$$

In the first and second parts of Eqs.(12)-(13), the *gravitational* versus the *inertial* contributions to the change in energy and momentum density are apparent. Substitutions from (11) into (12)-(13) result in the invariant forms of conservation equations [6]

$$\frac{\partial \rho_\beta}{\partial t} + \mathbf{w}_\beta . \nabla \rho_\beta - D_\beta \nabla^2 \rho_\beta = \Omega_\beta \tag{14}$$

$$\frac{\partial T_\beta}{\partial t} + \mathbf{w}_\beta . \nabla T_\beta - \alpha_\beta \nabla^2 T_\beta = -h_\beta \Omega_\beta / (\rho_\beta c_{p\beta}) \tag{15}$$

$$\frac{\partial \mathbf{v}_\beta}{\partial t} + \mathbf{w}_\beta . \nabla \mathbf{v}_\beta - \nu_\beta \nabla^2 \mathbf{v}_\beta = -\mathbf{v}_\beta \Omega_\beta / \rho_\beta \tag{16}$$

An important feature of the modified equation of motion (16) is that it involves a convective velocity $\mathbf{w}_\beta$ that is different from the local fluid velocity $\mathbf{v}_\beta$. Because the convective velocity $\mathbf{w}_\beta$ is not *locally defined* it cannot occur in *differential form* within the conservation equations [5]. This is because one cannot differentiate a function that is not locally, i.e. differentially, defined. To determine $\mathbf{w}_\beta$, one needs to go to the next higher scale (β+1) where $\mathbf{w}_\beta = \mathbf{v}_{\beta+1}$ becomes a local velocity. However, at this new scale one encounters yet another convective velocity $\mathbf{w}_{\beta+1}$ which is not known, requiring consideration of the higher scale (β+2). This unending chain constitutes the *closure problem* of the statistical theory of turbulence discussed earlier [5].

3 Connection Between the Modified Form of the Equation of Motion and the Navier-Stokes Equation

The original form of the *Navier-Stokes* equation with constant coefficients is given as [1, 2]

$$\rho\frac{\partial \mathbf{v}}{\partial t}+\rho\mathbf{v}.\nabla\mathbf{v}=-\nabla P+\mu\nabla^2\mathbf{v}+\frac{1}{3}\mu\nabla(\nabla.\mathbf{v}) \quad (17)$$

Since thermodynamic pressure P_t is an isotropic scalar, P in (17) is not P_t. Rather, the pressure P is generally identified as the *mechanical pressure* that is defined in terms of the total stress tensor $T_{ij}=-P_t\delta_{ij}+\tau_{ij}$ as [7]

$$P_m=-(1/3)T_{ii}=P_t-(1/3)\tau_{ii} \quad (18)$$

The normal viscous stress is given by (10) as $(1/3)\tau_{ii}=(1/3)\rho\mathbf{v}_i\mathbf{V}_{ii}=-(1/3)\mu\nabla.\mathbf{v}$ and since $\nabla P_t\approx 0$ because of isotropic nature of P_t, the gradient of (18) becomes

$$\nabla P=\nabla P_m=\nabla\frac{1}{3}\mu(\nabla.\mathbf{v})=\frac{1}{3}\mu\nabla(\nabla.\mathbf{v}) \quad (19)$$

Substituting from (19) into (17), the *Navier-Stokes* equation assumes the form

$$\frac{\partial \mathbf{v}}{\partial t}+\mathbf{v}.\nabla\mathbf{v}-\nu\nabla^2\mathbf{v}=0 \quad (20)$$

that is almost identical to (16) with $\Omega_\beta=0$ except that in (16) the convective velocity $\mathbf{w}_\beta$ is different from the local velocity $\mathbf{v}_\beta$. However, because (20) includes a diffusion term and $\mathbf{w}_\beta$ and $\mathbf{v}_\beta$ are related by $\mathbf{v}_\beta=\mathbf{w}_\beta+\mathbf{V}_\beta$, it is clear that (20) should in fact be written as (16).

4 Solution of the Modified Equation of Motion within Laminar Boundary Layer Adjacent to an Axi-Symmetric Stagnation-Point

As two examples of exact solutions of the modified equation of motion (16), the classical problems of two-dimensional and axi-symmetric jets [2] for laminar [8] and turbulent [9] flow were recently introduced. In this section, the solution of the modified equation of motion (16) for the classical problem of laminar flow within the boundary layer adjacent to an axi-symmetric stagnation-point is considered. The convective velocity field (w'_{rc}, w'_{zc}) outside of the boundary layer, schematically shown in Fig.2, is known and given by [2]

$$w'_{rc}=\Gamma_c r'_c \qquad w'_{zc}=-2\Gamma_c z'_c \quad (21)$$

where Γ_c is the velocity gradient and the subscript (c) refers to the laminar cluster-dynamic (LCD) scale β = c [5]. The convective velocity field (21) itself and hence Γ_c will be determined in the following section from the solution of the modified equation of motion (16) for axi-symmetric laminar finite-jet stagnation-point flow and counterflow configurations at the next larger scale of laminar eddy–dynamics (LED) β = e [5]. In this section the *local* radial and axial velocities within the thin boundary layer adjacent to the wall at the scale β = c will be examined.

For laminar eddy-dynamics, the dissipative length scale is the cluster size $l_c\approx\lambda_m=10^{-7}$ m i.e. the free path of molecular clusters. Also, a typical element size is $\lambda_c=L_m\approx 10^{-2}$ mm. Finally, a typical LCD system length is $L_c\approx 1$ mm that is of the order of the boundary layer thickness. The relevant kinematic viscosity at this scale is estimated as [5]

$$\nu_c=l_c u_c/3=\lambda_m v_m/3 \approx\frac{1}{3}(10^{-7}\,\text{m}\times 300\ \text{m/s})=0.1\ \text{cm}^2/\text{s} \quad (22)$$

where v_m is the mean thermal speed of molecules. The notation $(v'_{rc},\ v'_{zc})$ is chosen for the *local* radial and axial velocities along the corresponding coordinates $(r'_c,\ z'_c)$.

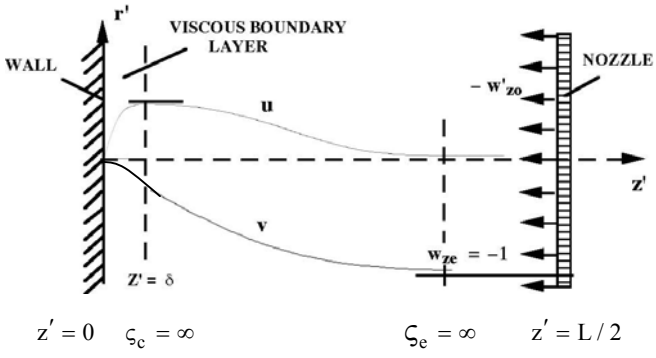

Fig.2 Laminar finite-jet axi-symmetric stagnation-point flow ($u = v_{rc}$, $v = v_{zc}$).

Under the conventional boundary layer assumptions $\partial / \partial r_c' \ll \partial / \partial z_c'$, and $\partial^2 / \partial r_c'^2 \ll \partial^2 / \partial z_c'^2$ and with introduction of the dimensionless velocities

$$(\mathbf{v_{rc}}, \mathbf{v_{zc}}, \mathbf{w_{zc}}) = (\mathbf{v'_{rc}}, \mathbf{v'_{zc}}, \mathbf{w'_{zc}}) / \sqrt{\nu_c \Gamma_c} \qquad (23)$$

and coordinates

$$\xi_c = r_c' / \delta_c \ , \quad \varsigma_c = z_c' / \delta_c \ , \quad \delta_c = \sqrt{\nu_c / \Gamma_c} \qquad (24)$$

the steady forms of (14) and (16) in the absence of chemical reactions $\Omega = 0$ reduce to

$$\frac{\partial v_{zc}}{\partial \varsigma_c} + \frac{\partial v_{rc}}{\partial \xi_c} + \frac{v_{rc}}{\xi_c} = 0 \qquad (25)$$

$$w_{zc} \frac{\partial v_{rc}}{\partial \varsigma_c} = \frac{\partial^2 v_{rc}}{\partial \varsigma_c^2} \qquad (26)$$

$$w_{zc} \frac{\partial v_{zc}}{\partial \varsigma_c} = \frac{\partial^2 v_{zc}}{\partial \varsigma_c^2} \qquad (27)$$

that are subject to the boundary conditions

$$\varsigma_c = 0 \qquad v_{rc} = v_{zc} = 0 \qquad (28)$$

$$\varsigma_c \to \infty \qquad v_{rc} = w_{rc} = \xi_c$$

$$dv_{zc} / d\varsigma_c = dw_{zc} / d\varsigma_c = -2 \qquad (29)$$

Because usually $\sqrt{\nu_c / \Gamma_c} \ll \mathbf{1}$, the boundary layer coordinates (ξ_c , ζ_c) in (24) are stretched coordinates. According to (29), the quantities (v_{rc}, $dv_{zc}/d\zeta_c$) within the boundary layer are matched with the outer convective velocity fields (w_{rc}, $dw_{zc}/d\zeta_c$) from (21) in the limit $\varsigma_c \to \infty$ (Fig.2). The presence of boundary layer results in the displacement of the outer flow field (21) towards the nozzle to be further discussed in the next section.

Following the classical methods [2, 9, 10], an approximate similarity solution of the form

$$v_{rc} = \xi_c f(\varsigma_c) \qquad (30)$$

is considered for the radial velocity and the corresponding axial velocity is directly determined from the continuity equation (25). Therefore, the exact solutions of (25)-(26), that do not satisfy (27) and hence represent an approximate solution of the problem, expressed in terms of the stream function

$$\Psi_c = -\xi_c^2 \int_0^{\varsigma_c} \mathrm{erf}(y)\,dy \qquad (31)$$

are

$$v_{rc} = -\frac{1}{\xi_c} \frac{\partial \Psi_c}{\partial \varsigma_c} = \xi_c \mathrm{erf}(\varsigma_c) \qquad (32)$$

$$v_{zc} = \frac{1}{\xi_c} \frac{\partial \Psi_c}{\partial \xi_c} = -2 \int_0^{\varsigma_c} \mathrm{erf}(y)\,dy \qquad (33)$$

The streamlines calculated from (31) and shown in Fig.3 are in accordance with observations and appear similar to those presented in Fig.5.9 of *Schlichting* [2] for stagnation in plane flow.

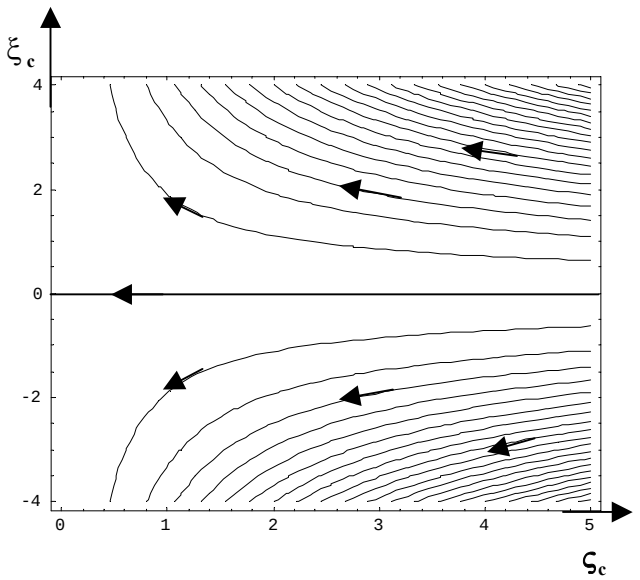

Fig.3 Calculated streamlines from (31) for stagnation-point boundary layer flow.

The predicted velocity profiles calculated from (32) and (33) with $(1/\pi^{1/2})$ due to the strain rate from (79) is shown in Fig.4. The predicted radial velocity (32) is in excellent quantitative agreement with the classical numerical results of *Homann* [10] and *Frössling* [11] presented in Fig.5.10 of *Schlichting* [2]. On the other hand, while the agreement between the predicted axial velocity (33) and the classical numerical result [2, 10, 11] is good near the wall, the two solutions deviate far away from the wall. However, the far field behavior of the modified

solution (33) must be determined by matching to the outer solutions at LED scale to be described in the following section. The exact comparisons between the predictions and the experimental observations as well as the exact numerical calculations require future considerations.

The dimensionless axial coordinate (24) may also be expressed as

$$\varsigma_c = z'_c / \sqrt{\nu_c / \Gamma_c} = \frac{z'}{L_c}\sqrt{\frac{w'_{zc} L_c}{\nu_c}} = z_c \sqrt{Re_c} \qquad (34)$$

showing explicitly the coordinate stretching by $\sqrt{Re_c}$. It is emphasized however that neither L_c nor w'_{zc} are *a-priori* known parameters of the problem and hence cannot be used to non-dimensionalize quantities. The predicted boundary layer thickness defined as the position where $v_{rc} = v'_{rc} / w'_{rc} \approx 0.9995$ is obtained from (32) as

$$\varsigma_{c\infty} \approx 2.4 \quad , \quad z'_{c\infty} = 2.4\sqrt{\nu_c / \Gamma_c} \qquad (35)$$

in exact agreement with the classical numerical calculations [2, 9, 10].

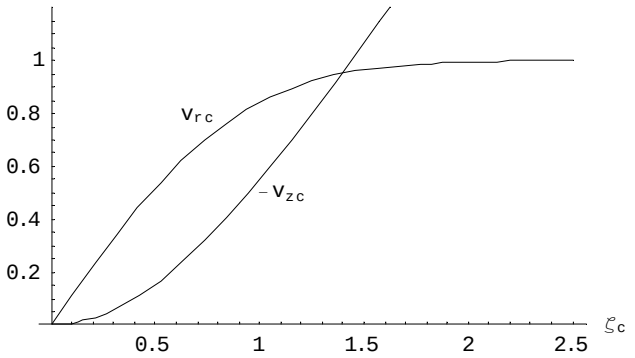

Fig.4 Calculated axial and radial velocity profiles within the boundary layer from (32)-(33).

The choice of 2.4 in (35) is to facilitate comparisons with the classical studies [2]. However, according to the predicted velocity profile of the present theory in (32), the edge of the boundary layer is already reached to an accuracy of 0.995 at

$$\varsigma^*_c \approx 2.0 \qquad (36)$$

and this modified value will be more relevant to the scaling process to be discussed in the next section. Also, one notes that the boundary layer thickness ς^*_c in (36) is four times the length to the position ζ_{co} = 1/2 where the asymptotic profile of the axial velocity v_{ze} crosses the abscissa in Fig.4.

The dimensional hydrodynamic boundary layer thickness from (36) and (24) is

$$\ell_c = z'^*_c = \frac{2.0 L_c}{\sqrt{Re_c}} \qquad (37)$$

For a typical laboratory-scale experiment [13] with $L_c \approx 2$ mm, $w'_{zc} \approx 2$ cm/s, and $\nu_c \approx 0.1$ cm^2/s for air, one obtains the strain rate $\Gamma_c = w'_{zc} / L_c \approx 10$ s^{-1} and $Re_c = (w'_{zc} L_c)/\nu_c = 4$, such that (37) leads to $\ell_c \approx 2.0$ mm that is indeed of the order of L_c for laminar cluster-dynamic scale. Therefore, as suggested earlier, typical lengths for the description of the entire structure of the boundary layer at LCD scale are about ($l_c = 10^{-7}$, $\lambda_c = 10^{-5}$, $L_c = 10^{-3}$) m.

5 Solution of the Modified Equation of Motion Outside of the Boundary Layer of Axi-symmetric Stagnation-Point Flow or the Free Viscous Layer of Counterflow Finite Jets

According to the scale-invariant form of the equation of motion (16) the convective velocity (w'_{rc}, w'_{zc}) at laminar cluster-dynamic (LCD) scale $\beta = c$ is the local velocity (v'_{re}, v'_{ze}) at the next higher scale of laminar eddy-dynamics (LED) $\beta = e$. Therefore, in this section the velocities (w'_{rc}, w'_{zc}) given in (21) are determined from the solution of (16) at scale $\beta = e$, outside of the boundary layer of a finite-jet stagnation-point flow shown in Fig.2. In addition, the solution of equation of motion outside of free-viscous-layer within an axi-symmetric finite-jet counterflow schematically shown in Fig.5 will be described.

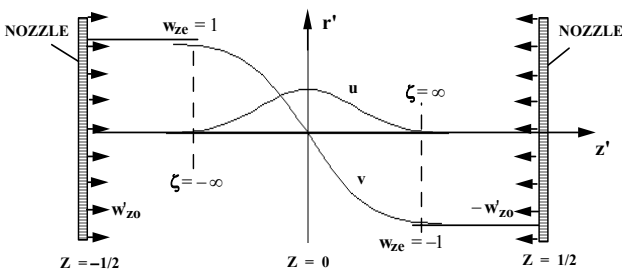

Fig.5 Calculated velocity profiles for axi-symmetric finite-jet counterflow ($u = v_{re}$, $v = v_{ze}$) from (74)-(75).

The relevant ("atomic", element, system) lengths [5] at laminar eddy-dynamic (LED) scale are ($l_e = 10^{-5}$, $\lambda_e = 10^{-3}$, $L_e = 10^{-1}$ m) and the actual lengths relevant to typical laboratory-scale experiments will be about (0.1, 1, 100) mm. Also, the relevant kinematic viscosity for the scale $\beta = e$ is estimated as [5]

$$\nu_e = l_e u_e / 3 = \lambda_c v_c / 3 \approx \frac{1}{3}(10^{-5}\,\mathrm{m} \times 3\,\mathrm{m/s}) = 0.1\,\mathrm{cm^2/s} \qquad (38)$$

indicating that motions dissipate into the "atomic" scale of LED that is the same as the "elemental" scale of LCD [5]. The general form of the solutions for axial and radial velocity fields outside of the stagnation-point boundary layer shown in Fig.2 are expected to be similar to those outside of the free-viscous-layer of finite-jet counterflow shown in Fig.5. The free viscous layer in Fig.5 is a thin dissipative layer at LCD scale that is embedded within the outer "boundary layer" at LED scale.

The conventional boundary layer assumptions $\partial / \partial r'_e \ll \partial / \partial z'_e$, $\partial^2 / \partial r'^2_e \ll \partial^2 / \partial z'^2_e$ are made and the dimensionless quantities

$$(\mathbf{v_r}, \mathbf{v_z}, \mathbf{w_{ze}}) = (\mathbf{v'_r}, \mathbf{v'_z}, \mathbf{w'_{ze}}) / \mathbf{w'_{zeo}}$$

$$r_e = r'_e / L_e \quad , \quad z_e = z'_e / L_e \qquad (39)$$

are introduced where w'_{zeo} is the given axial convective velocity at the nozzle and L_e is twice the separation distance between the nozzle and the wall (Fig.2) or the separation distance between the opposing nozzles (Fig.5). The steady forms of (14) and (16) at LED scale $\beta = e$ [5] in the absence of chemical reactions $\Omega = 0$ reduce to

$$\frac{\partial v_z}{\partial z_e} + \frac{\partial v_r}{\partial r_e} + \frac{v_r}{r_e} = 0 \qquad (40)$$

$$w_{ze} \frac{\partial v_r}{\partial z_e} = \frac{1}{Re_e} \frac{\partial^2 v_r}{\partial z_e^2} \qquad (41)$$

$$w_{ze} \frac{\partial v_z}{\partial z_e} = \frac{1}{Re_e} \frac{\partial^2 v_z}{\partial z_e^2} \qquad (42)$$

where the Reynolds number

$$Re_e = \frac{w'_{zeo} L_e}{\nu_e} \qquad (43)$$

is based on the kinematic viscosity ν_e defined in (38). The equations (40)-(42) are subject to the boundary conditions

$$z_e = 1/2 \qquad v_r = v_z + 1 = 0$$
$$z_e \to \ell_c \qquad \partial v_r / \partial z = \partial v_{ze} / \partial z_e - \partial v_{zc} / \partial \varsigma_c = 0 \qquad (44)$$

for the finite-jet stagnation-point flow (Fig.2) and

$$z_e = 1/2 \qquad v_r = v_z + 1 = 0$$
$$z_e = 0 \qquad \partial v_r / \partial z_e = v_z = 0 \qquad (45)$$
$$z_e = -1/2 \qquad v_r = v_z - 1 = 0$$

for the finite-jet counterflow (Fig.5).

In the "inviscid" limit $Re_e \to \infty$ far away from the stagnation plane $z_e = 0$, (41)-(42) simplify to the convective terms only thus leading to the outer solutions

$$1/2 > z_e >> 0 \quad v_r = v_z + 1 = w_{ze} + 1 = 0 \qquad (46)$$

Therefore, far away from the stagnation plane the jet velocity is purely axial because the presence of the stagnation plane has not yet induced any jet divergence as shown in Fig.2.

Next, for the analysis of the "viscous" solution at the LED scale, parallel to (23)-(24), one introduces the stretched velocities and coordinates as

$$(\mathbf{v_{re}}, \mathbf{v_{ze}}, \mathbf{w_{ze}}) = (\mathbf{v'_{re}}, \mathbf{v'_{ze}}, \mathbf{w'_{ze}}) / \sqrt{\nu_e \Gamma_e} \qquad (47)$$

$$\varsigma_e = z'_e / \delta_e \quad , \quad \xi_e = r'_e / \delta_e \quad , \quad \delta_e = \sqrt{\nu_e / \Gamma_e} \qquad (48)$$

where

$$\Gamma_e = \frac{w'_{zeo}}{L_e} \qquad (49)$$

The axial convective velocity w_{ze} that satisfies the boundary conditions (44) is given by

$$w'_{ze} = -2\Gamma_e (z'_e - \delta_e / 2) \qquad (50)$$

that includes the apparent displacement of the position of the stagnation plane due to the presence of the viscous boundary layer. Substituting from (47) and (48) into (50) leads to

$$w_{ze} = -(2\varsigma_e - 1) \qquad (51)$$

Assumptions $\partial/\partial r_e' \ll \partial/\partial z_e'$, $\partial^2/\partial r_e'^2 \ll \partial^2/\partial z_e'^2$ and substitutions from (47), (48) and (50) into (14)-(16) with $\Omega = 0$ result in

$$\frac{\partial v_{ze}}{\partial \varsigma_e} + \frac{\partial v_{re}}{\partial \xi_e} + \frac{v_{re}}{\xi_e} = 0 \tag{52}$$

$$\frac{\partial^2 v_{re}}{\partial \varsigma_e^2} + (2\varsigma_e - 1)\frac{\partial v_{re}}{\partial \varsigma_e} = 0 \tag{53}$$

$$\frac{\partial^2 v_{ze}}{\partial \varsigma_e^2} + (2\varsigma_e - 1)\frac{\partial v_{ze}}{\partial \varsigma_e} = 0 \tag{54}$$

The stretched coordinates in (24) and (48) lead to the general expression

$$\varsigma_\beta = \frac{z'}{\delta_\beta} \tag{55}$$

such that the LCD and the LED coordinates $(\varsigma_\beta,\ \varsigma_{\beta+1}) = (\varsigma_c,\ \varsigma_e)$ could be made to become "numerically equivalent" by proper choice of the scales $(\delta_c,\ \delta_e)$. According to the analysis of the boundary layer in the previous section at LCD scale $(l_c = 10^{-7},\ \lambda_c = 10^{-5},\ L_e = 10^{-3})$ m the boundary layer thickness and the characteristic length are related as $\varsigma_{co} = \varsigma_c^* / 4 = \ell_c / 4 = L_c / 4$ such that $\lambda_c = L_c / 4$. One requires that the characteristic elemental length of LED match the system length L_c of LCD $\lambda_e = L_c$ leading to the LED length scales $(l_e = 10^{-5},\ \lambda_e = 10^{-3},\ L_e = 10^{-1})$ m. Therefore, the characteristic unit lengths of the two boundary layer thicknesses $(\delta_c,\ \delta_e)$ will be related by

$$\delta_e = 4\delta_c \tag{56}$$

that by (24), (48), and (56) result in

$$\varsigma_e = \varsigma_c / 4 \quad , \quad \xi_e = \xi_c / 4 \tag{57}$$

Substituting from (57) into (52)-(54) and introducing the new axial and radial coordinates

$$y_e = (1/2)[\varsigma_c / 2 - 1] \quad , \quad x_e = \xi_c / 4 \tag{58}$$

result in the system

$$\frac{\partial v_{ze}}{\partial y_e} + \frac{\partial v_{re}}{\partial x_e} + \frac{v_{re}}{x_e} = 0 \tag{59}$$

$$\frac{\partial^2 v_{re}}{\partial y_e^2} + 2y_e \frac{\partial v_{re}}{\partial y_e} = 0 \tag{60}$$

$$\frac{\partial^2 v_{ze}}{\partial y_e^2} + 2y_e \frac{\partial v_{ze}}{\partial y_e} = 0 \tag{61}$$

that are subject to the boundary conditions

$$y_e \to \infty \quad v_{re} = v_{ze} + 1 = 0 \tag{62a}$$

$$y_e = 0 \quad \partial v_{re}/\partial y_e = \partial v_{ze}/\partial y_e - \partial v_{zc}/\partial \varsigma_c = 0 \tag{62b}$$

The system (59)-(61) that describes the outer LED flow field involves the same coordinate ζ_c of the inner LCD boundary layer discussed in the previous section.

Following the classical studies [2, 9, 10], but as opposed to the *radial* velocity (30) chosen for the solution within the boundary layer discussed in sec.4, one now considers the *axial* velocity to have an approximate similarity solution of the form

$$v_{ze} = -g(y_e) \tag{63}$$

and the corresponding radial velocity $v_{re} = x_e g'(y_e)/2$ is determined from the continuity equation (59). Hence, the exact solutions of (59) and (61), will not satisfy (60) and hence represent approximate solutions of the problem. The solution of (61)-(62) is given as

$$v_{ze} = -\frac{1}{A}\int_{1/2}^{\varsigma_c} \exp[-0.25(\varsigma_c / 2 - 1)^2]\, d\varsigma_c \tag{64}$$

where the constant A is defined as

$$A = \int_{1/2}^{\infty} \exp[-0.25(\varsigma_c / 2 - 1)^2]\, d\varsigma_c = 4.97746 \tag{65}$$

After substitution from (61) into the continuity equation (59) the radial velocity outside of the boundary layer is obtained as

$$v_{re} = \frac{\xi_c \exp[-0.25(\varsigma_c / 2 - 1)^2]}{2A} \tag{66}$$

The corresponding solutions within the boundary layer that are matched to the outer solutions (64) and (66) are obtained from (32) and (33) as

$$v_{rc} = (\xi_c / 2A)\ \mathrm{erf}(\varsigma_c) \tag{67}$$

and

$$v_{zc} = -(1/A)\int_0^{\varsigma_c} \mathrm{erf}(\varsigma_c)\, d\varsigma_c \tag{68}$$

The predicted velocity profiles calculated from (64)-(68) are shown in Fig.6 and are in accordance with the classical results [2]. The exact comparisons of the predicted velocity profiles in Fig.6 with the available experimental observations in the literature will require future considerations.

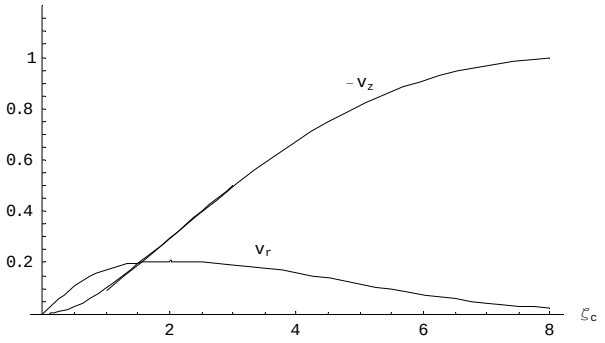

Fig.6 Laminar axi-symmetric stagnation-point flow inside and outside of the boundary layer.

Finally, the problem of two axi-symmetric counterflow finite jets forming a thin free viscous layer at the stagnation plane shown in Fig.5 is addressed. The solution of system (52)-(54) with the boundary conditions (45) will become very simple if one assumes that the *inner* viscous layer has zero thickness, i.e. the LCD viscosity given in (22) vanishes $\nu_c = 0$. It is emphasized here that only the thickness of the inner free viscous layer at LCD scale is assumed to vanish, $\delta_c = 0$, while the viscosity at LED scale ν_e and hence δ_e in (48) is considered to remain finite. Under such an assumption, the thickness of free-viscous layer vanishes and the convective velocity (51) reduces to

$$w_{ze} = -2\varsigma_e \tag{69}$$

such that (52)-(54) become

$$\frac{\partial v_{ze}}{\partial \varsigma_e} + \frac{\partial v_{re}}{\partial \xi_e} + \frac{v_{re}}{\xi_e} = 0 \tag{70}$$

$$\frac{\partial^2 v_{re}}{\partial \varsigma_e^2} + 2\varsigma_e \frac{\partial v_{re}}{\partial \varsigma_e} = 0 \tag{71}$$

$$\frac{\partial^2 v_{ze}}{\partial \varsigma_e^2} + 2\varsigma_e \frac{\partial v_{ze}}{\partial \varsigma_e} = 0 \tag{72}$$

The solutions of (70)-(72) and (45) expressed in terms of the stream function

$$\Psi_e = -\frac{\xi_e^2}{2}\mathrm{erf}(\varsigma_e) \tag{73}$$

are

$$v_{ze} = -\mathrm{erf}(\varsigma_e) \tag{74}$$

$$v_{re} = \frac{\xi_e}{\sqrt{\pi}}\exp(-\varsigma_e^2) \tag{75}$$

The calculated streamlines for the outer LED scale calculated from (73) are shown in Fig.7 and are to be compared with the streamlines within the viscous boundary layer at LCD scale shown in Fig.3.

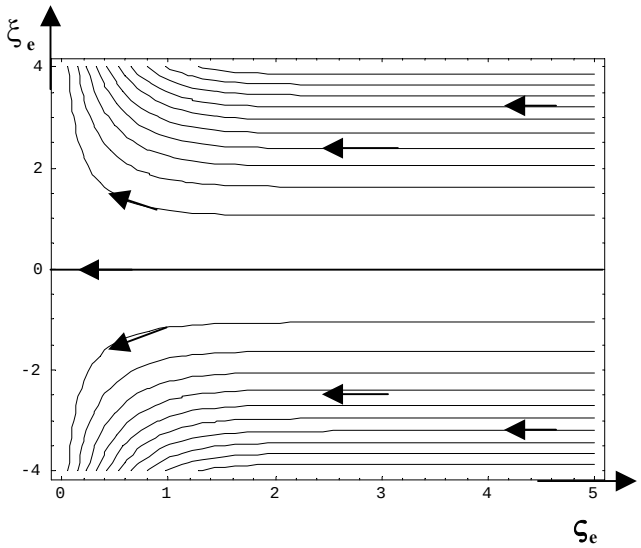

Fig.7 Calculated streamlines from (73) for outer LED scale finite-jet stagnation-point flow.

The axial and radial velocity profiles calculated from (74)-(75) are shown in Fig.5 and are in qualitative agreement with experimental observations [14, 15].

In particular, the predicted behavior of the axial velocity across the stagnation plane shown in Fig.5 is in accordance with the experimental observations of *Yamaoka and Tsuji* [14].

The local velocity (v'_{re}, v'_{ze}) at LED scale in (74)-(75) also represent the convective velocity (w'_{rc} , w'_{zc}) at the next lower scale of LCD. In the neighborhood of the stagnation plane, $\varsigma_e \ll 1$, the solutions (74)-(75) lead to

$$v_{ze} = -\frac{2}{\sqrt{\pi}}\varsigma_e \quad , \quad v_{re} = \frac{1}{\sqrt{\pi}}\xi_e \qquad (76)$$

that in view of (47) and (48) could be expressed as

$$v'_{ze} = w'_{zc} = -\frac{2}{\sqrt{\pi}}\Gamma_e z' = -2\Gamma_c z' \qquad (77)$$

$$v'_{re} = w'_{rc} = \frac{\Gamma_e}{\sqrt{\pi}} r' = \Gamma_c r' \qquad (78)$$

if one introduces the following new definition

$$\Gamma_c = \frac{\Gamma_e}{\sqrt{\pi}} \qquad (79)$$

The results (77)-(78) are identical to the convective velocity field (21) of sec.3. The application of the results to the important problem of combustion in stagnation flows [3, 12-16] requires future considerations.

6 Concluding Remarks

The modified form of the equation of motion was solved for the classical problems of laminar incompressible flow within boundary layer adjacent to an axi-symmetric stagnation-point and laminar flow outside of the free viscous layer at the stagnation plane between axi-symmetric counterflow finite jets. For the former problem, the resulting analytical solution for radial velocity was found to be in excellent agreement with the exact numerical calculations of *Homann* and *Frössling.* The predicted axial velocity showed close agreement with the classical numerical results near the wall, but the two solutions deviated far away from the wall. For the latter problem, the predicted behavior of the axial velocity profile across the stagnation plane was found to be in agreement with the experimental observations of *Yamaoka and Tsuji*.

References :

[1] de Groot, R. S., and Mazur, P., *Nonequilibrium Thermodynamics*, North-Holland, 1962.

[2] Schlichting, H., *Boundary-Layer Theory*, McGraw Hill, New York, 1968.

[3] Williams, F. A., *Combustion Theory*, 2nd Ed., Addison-Wesley, New York, 1985.

[4] Sohrab, S. H., *Rev. Gén. Therm.* **38**, 845-854 (1999).

[5] Sohrab, S. H., Transport phenomena and conservation equations for multi-component chemically reactive ideal gas mixtures. *Proceeding of the 31st ASME National Heat Transfer Conference*, HTD Vol. **328**, 37-60 (1996).

[6] Sohrab, S. H., WSEAS *Transactions on Mathemathics*, Issue **4**, Vol.3, 755 (2004).

[7] Panton, R. L., *Incompressible Flow*, Wiley, New York, 1996.

[8] Sohrab, S., H., *IASME Transactions* **3**, Vol.1, 466 (2004).

[9] Sohrab, S., H., *IASME Transactions* **4**, Vol.1, 626 (2004).

[10] Homann, F., Der Einfluβ groβer Zähigkeit bei der Strömung um den Zylinder und um die Kugel. *ZAMM* **16**, 153-164 (1936); *Forschg. Ing.-Wes.***7**, 1-10 (1936).

[11] Frössling, N., Verdunstung, Wärmeübertragung und Geschwindigkeitsverteilung bei zweidimensionaler und rotationssymmetrischer laminarer Grenzschichtströmung. Lunds. Univ. Arsskr. N. F. Avd. 2, **35**, No.4 (1940).

[12] Liñán, A., The asymptotic structure of counterflow diffusion flames for large activation energies. *Acta Astronautica* **1**:1007 (1974).

[13] Warnatz, J., Maas, U., and Dibble, R. W., *Combustion,* Springer, New York, 1996.

[14] Yamaoka, I., and Tsuji, H., An experimental study of flammability limits using counterflow flames. *Proc. Combust. Inst.***17**, 843 (1978).

[15] Chen, Z. H., Liu, G. E., and Sohrab, S. H., *Combust. Sci. Technol.* **51**, 39 (1987).

[16] Sohrab, S. H., Ye, Z. Y., Law, C. K., *Combust. Sci. Technol.* **45**, 27 (1986).